On 3G LTE Terminal Implementation – Standard, Algorithms, Complexities and Challenges

Jens Berkmann, Cecilia Carbonelli, Frank Dietrich, Christian Drewes, Wen Xu
Infineon Technologies AG
Am Campeon 1-12, 85579 Neubiberg, Germany
first_name.last_name@infineon.com
(Invited Paper)

***Abstract*—Currently, 3GPP standardizes an evolved UTRAN (E-UTRAN) within the Release 8 Long Term Evolution (LTE) project. Targets include higher spectral efficiency, lower latency, higher peak data rate when compared to previous 3GPP air interfaces. The air interface of E-UTRAN is based on OFDMA and MIMO in downlink and on SCFDMA in uplink. Main challenges for a terminal implementation include efficient realization of the inner receiver, especially for channel estimation and equalisation, and the outer receiver including a turbo decoder which needs to handle data rates of up to 75 Mbps per spatial MIMO stream. We show that the inner receiver can nicely and straightforwardly be parallelized due to frequency domain processing. In addition to the computational complexity of even a simple linear equaliser, one of the challenges is an efficient implementation considering necessary flexibility for different MIMO modes, power consumption and silicon area. This paper will briefly overview the current LTE standard, highlight a functional data flow through the single entities of an LTE terminal and elaborate more on possible first implementation details, including sample algorithms and first complexity estimates.**

***Index Terms* — 3GPP LTE, OFDM, MIMO, receiver design**

I. INTRODUCTION

THE mobile radio network technology family of the 3GPP (3rd Generation Partnership Project) as well as its predecessor ETSI (European Telecommunications Standards Institute), including GSM/EDGE (Global System for Mobile communications/Enhanced Data rate for GSM Evolution) and UMTS/HSPA (Universal Mobile Telecommunication System/High Speed Packet Access) technologies, now accounts for over 85% of all mobile subscribers worldwide. The further increasing demand on high data rates in new applications such as mobile TV, online gaming, multimedia streaming, etc., has motivated the 3GPP to work on the long term evolution (LTE) project since late 2004. Overall target was to select and specify technology that would keep 3GPP's technologies at the forefront of mobile wireless well into the next decade.

Key objectives of the 3GPP LTE, whose radio access is called Evolved UMTS Terrestrial Radio Access Network (E-UTRAN), include substantially improved end-user throughputs, sector capacity, reduced user plane latency, significantly improved user experience with full mobility, simplified lower-cost network and reduced User Equipment (UE) complexity. Currently, first 3GPP LTE specification is being finalized within 3GPP Rel-8. Specifically, the physical layer has become quite stable recently for a first implementation.

The air interface of E-UTRAN is based on OFDMA (Orthogonal Frequency Division Multiple Access) and MIMO (Multiple-Input Multiple Output) in downlink (DL) and on SCFDMA (Single Carrier Frequency Division Multiple Access) in uplink (UL) direction. Main challenges for a terminal implementation include efficient realization of the inner receiver, especially for channel estimation and equalisation, and the outer receiver including a turbo decoder which needs to handle data rates of up to 75 Mbps per spatial MIMO stream. We show that the inner receiver can nicely and straightforwardly be parallelized due to frequency domain processing. In addition to the pure computational complexity of even a simple linear equaliser, one of the challenges is an efficient implementation considering necessary flexibility for different MIMO modes, low power consumption and small silicon area.

This paper is structured as follows: In section II, we first give a brief overview of the 3GPP LTE system, especially the physical layer. An example LTE UE implementation including the core functional algorithms of the baseband processing data flow is described in section III. In section IV we will evaluate the computational and memory requirements for an example implementation, and highlight the challenges. Finally, some concluding remarks are given in section V.

II. OVERVIEW OF THE 3GPP LTE

The 3GPP LTE physical layer is responsible to convey data and control information between an LTE base station called eNB (evolved Node B) and the UE. The LTE has been designed to meet, among others, the following physical layer requirements [1]

- *Bandwidth* scalable for 1.4, 3, 5, 10, 15, 20 MHz.
- *Antenna configuration*: Up to 4x4 DL MIMO. In UL only antenna selection is specified, i.e. a single spatial layer.
- *Peak data rate* scaling with bandwidth and number of spatial MIMO layers. Absolute peak rates are DL 300 Mb/s (4 layers) and UL 75 Mb/s (1 layer, 64-QAM) within 20 MHz bandwidth.

By using OFDM, LTE is in principle aligning with many IEEE 802 family standards, such as 802.16/WiMAX or 802.11/WiFi. However, within the 3GPP cellular standard family, OFDM based LTE is totally different from its predecessors such as time/frequency-division multiple-access based

978-1-4244-2202-9/08/$25.00

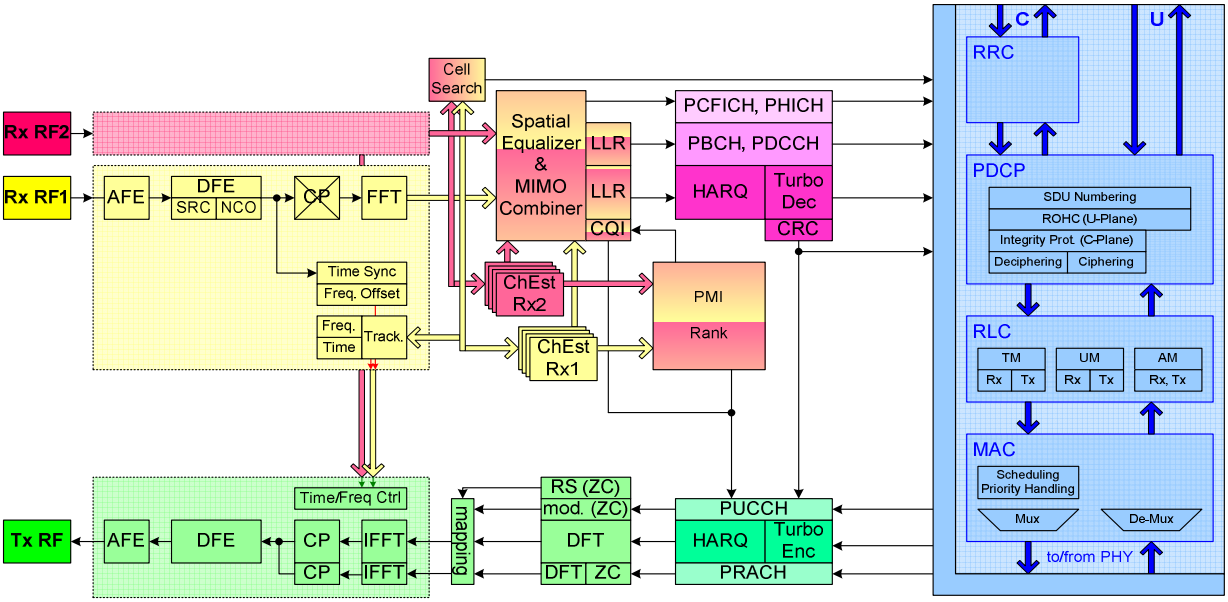

Fig. 1 Functional flow through an LTE terminal.

GSM/EDGE and code-division multiple-access based UMTS/HSPA. Except for a few techniques like turbo coding most implementations of existing 3GPP Rel-6 or Rel-7 physical layers cannot be reused.

LTE supports MIMO with one, two, and four antenna elements at eNB and UE. Both open and closed loop MIMO operation is possible. MIMO is coming in two flavours: transmit diversity (TD) maximizing diversity by transmitting dependent data over different antennas, and spatial multiplexing (SM) maximizing data rate by transmitting independent data over different antennas.

Precoding as a means of weighting the signals transmitted from different antennas in such a way that the signal-to-noise-plus-interference ratio (SNIR) at the receiver is maximized, is also adopted for LTE. Within LTE, precoding also comprises the operations required to arrive at TD schemes.

TD is based on the basic Alamouti diversity [5] applied on neighbouring subcarriers, i.e., a space frequency block code (SFBC). SM precoding with cyclic delay diversity (CDD) [6] has been removed from the standard recently. The codebook for SM with 4 transmit antennas is based on Householder reflections. Its elements are chosen to have a nested property, i.e., columns of precoding matrices for lower rank are a subset of those for higher rank. This allows for choosing a smaller rank at the base station and overruling the UE's rank and precoding matrix information feedback. Moreover, this property together with the Householder structure allows for complexity reduction in the algorithm selecting the best precoding matrix to be signalled back. The 2-antenna codebook is designed more intuitively without any special structure. For spatial multiplexing in an open loop mode a large delay CDD is added, which results in a periodic permutation between precoding matrices to reduce robustness to channel correlations. By scheduling multiple users onto different orthogonal layers of a codebook matrix multi-user MIMO can be deployed.

III. Physical Layer Signal Processing in a 3GPP LTE Terminal

Here, we only consider baseband processing and omit all analogue components, higher layer protocols and application processing. The functional block diagram in Fig. 1 shows an example of the internal data flows through an LTE UE with two receive (Rx) antennas and one transmit (Tx) antenna: The radio frequency (RF) signal is received by the receiver antennas, down converted, scaled by an automatic gain control, and digitized by an analogue to digital converter (ADC) within the analogue and digital frontends (AFE, DFE), including a sample rate converter (SRC) and a numerically controlled oscillator (NCO).

The baseband processor receives the digitized signal as complex samples from the ADCs and posts the decoded data stream to higher layer protocol and application processor: It first removes cyclic prefix (CP), transforms the signal into frequency domain by a fast Fourier transform (FFT), performs channel estimation, equalisation, log-likelihood-ratio (LLR) generation, hybrid automatic repeat request (HARQ) combining, channel decoding, and cyclic redundancy checking (CRC) for the different physical channels (P*CH): broadcast (PBCH), control format indicator (PCFICH), HARQ indicator (PHICH), downlink control (PDCCH), downlink shared (PDSCH). An explanation of all those different channels can be found in [2]. Additionally, control information for closed loop MIMO operation is generated: channel quality indication (CQI), precoding matrix information (PMI), and channel rank.

In uplink direction physical uplink shared channel (PUSCH) data gets encoded, Fourier transformed (DFT), and mapped onto single subcarriers together with a Zadoff-Chu (ZC) modulated physical uplink control channel (PUCCH) and ZC-modulated reference signals (RS). After inverse FFT (IFFT)

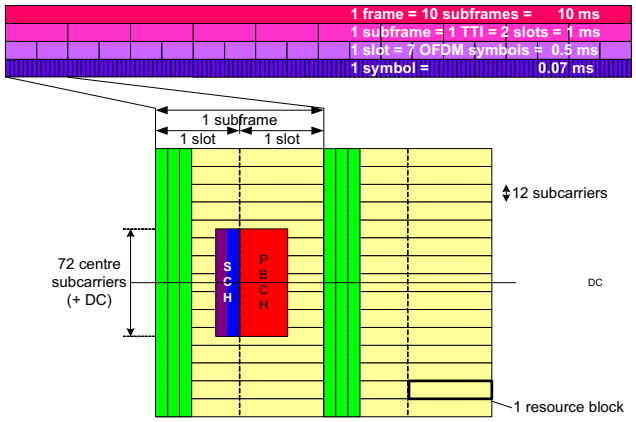

Fig. 2 3GPP LTE frame structure.

and CP appendix, data is sent to transmitter frontend and RF circuitry. For random access the corresponding physical random access channel (PRACH) is processed.

Protocol stack processing consists of medium access control (MAC) for scheduling different logical channels and multiplexing them onto transport channels, radio link control (RLC) with transparent, unacknowledged, and acknowledged modes (TM, UM, AM), packet data convergence protocol (PDCP) including ciphering, robust header compression (ROHC), and delivering service data units (SDU) from and to higher layers. Radio resource control (RRC) corresponds to layer 3 processing of control data, whereas MAC, RLC, ands PDCP build layer 2 [4].

Fig. 2 highlights some basic timing relations and the basic frame structure. The first up to three symbols in each subframe are reserved for control channels. Synchronization signals (SCH) are only transmitted in the first and eleventh slot of every frame. The PBCH is transmitted only in the second slot once per frame.

A. Synchronization and cell identification

In a typical receiver, synchronization is usually first conducted to acquire information such as the beginning of frame and the carrier frequency offset. After the acquisition phase the samples will be passed to the FFT, which translates the signal from time domain to frequency domain and simultaneously the inversion of OFDM is done. An overview on synchronization for OFDM can for instance be found in [7] and [8].

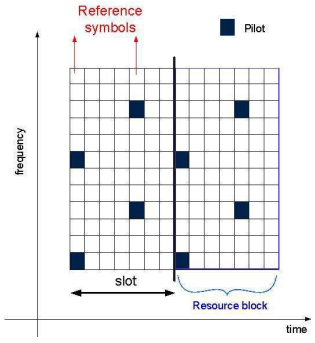

Fig. 3 Pilot grid for LTE SISO configuration.

In LTE, two synchronization signals are transmitted (primary and secondary), in the last two OFDM symbols of the first and eleventh slot in each radio frame. The primary signal is chosen from a variety of ZC sequences, carrying the information of the identity within a cell group. The secondary signal is a sequence carrying the information about the cell group, encoded with a scrambling sequence. After successful time and frequency synchronization, the cell identification can be performed.

B. Channel estimation

In LTE, like in many OFDM systems, known symbols, called *pilots*, are inserted at specific locations in the time-frequency grid in order to facilitate channel estimation. The resulting two-dimensional pilot pattern is typically irregular, as shown in Fig. 3 for the SISO case. It can be seen that the pilot spacing in frequency direction equals 6 subcarriers, while in time direction there are 2 OFDM symbols per slot (referred to as *reference symbols*) containing pilots, at a distance of 4 and 3 OFDM symbols from one another. Also, we recall that an LTE resource block in the downlink and with normal cyclic prefix is defined as a box containing 12 consecutive subcarriers and 7 consecutive OFDM symbols (Fig. 2), i.e., the resource block corresponds to one *slot* [2].

Channel estimates can first be obtained at the pilot positions using simple least squares demodulation, which for PSK pilot modulation reduces to a simple demodulation. The remaining channel coefficients can then be calculated using interpolation techniques in both time and frequency directions.

As for MIMO-OFDM, Fig. 4 illustrates the LTE pilot grid for a 2x2 antenna configuration. When antenna port 0 is transmitting its pilot symbols, the other antenna is silent. This implies that pilot transmissions from the two antenna ports are completely orthogonal, i.e., MIMO channel estimation is a straightforward extension of SISO channel estimation techniques.

There exist several approaches to two-dimensional (2D) pilot aided channel estimation for OFDM systems, where pilots are scattered on a time-frequency grid [9]. Among these, 2D Wiener interpolation has been often considered for practical receivers due to its robustness. In many cases, the 2D approach can be simplified with almost no loss in performance by resorting to a cascade type of estimator, often called 2x1D, where 2

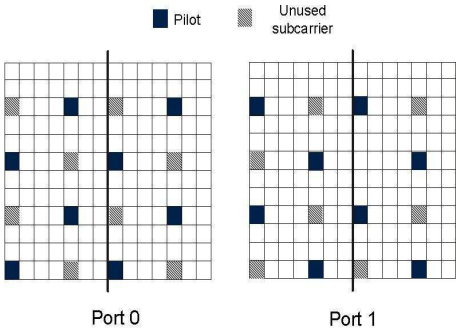

Fig. 4 Pilot grid for LTE 2x2 MIMO configuration.

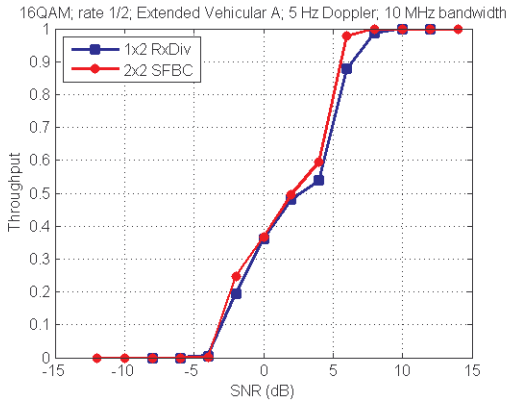

Fig. 5 Simulation results with realistic channel estimates for 1x2 Rx diversity and for 2x2 SFBC Tx diversity.

cascade orthogonal one-dimensional filters are employed.

Both 2D and 2x1D methods rely on minimal a priori channel knowledge. Usually, uniform Doppler and delay power spectra are assumed, where the limits are typically fixed to the maximum Doppler bandwidth and to the cyclic prefix length, respectively. This allows pre-computing the interpolation coefficients offline so that only multiplications by real-valued coefficients and summation operations are required in real time. Also, the minimum number of interpolating coefficients is typically $<< N$ (with N the size of the FFT) [9].

Fig. 5 shows some example throughput results with realistic channel estimates for the 1x2 Rx diversity (RxDiv) with maximum ratio combining, and for the 2x2 SFBC Tx diversity scenarios. The 5 Hz Doppler spread corresponds to a speed of about 3 km/h. The relative throughput is used here since the absolute throughput values usually differ for the RxDiv and SFBC scenarios, where a throughput of 100% means that *all* packets are correctly detected after HARQ processing.

C. Equalisation

Due to OFDM, equalisation may appear as a straightforward task. But, besides this simplification, the remaining challenge is the transmission of up to 4 spatial layers in a MIMO system on a maximum of 1200 subcarriers. Moreover, different equaliser designs are necessary to cover all transmission strategies and scenarios. Note also that the equaliser type can change on a subcarrier basis depending on the type of logical channel (data or control) assigned to it.

In contrast to the classic SISO, multiple Rx antennas and a single Tx antenna can provide valuable degrees of freedom which can be exploited by a matched filter to enhance the SNR and improve Rx diversity. Alternatively, a minimum mean square error (MMSE) combining can suppress strong inter-cell interference at the cell edge based on an estimate of the spatial noise-plus-interference correlation matrix. Note that the interference may vary from resource block to resource block depending on the scheduling in the neighbour cell.

A classic linear receiver is usually employed for the Alamouti-type orthogonal SFBC which is also used for several control and signalling channels. Thus, all 4 available spatial sources of diversity can be exploited in a 2x2 system.

A linear MMSE equaliser appears to be the first choice for separating the layers in the spatial multiplexing mode. The number of layers transmitted in parallel depends on the UE category: In the highest category 4 layers are possible, whereas category 2 to 4 allow only for 2 layers.

But linear equalisation cannot achieve a diversity order equal to the number of receive antennas. Thus, it is of high interest to improve throughput by fully taking advantage of MIMO in scenarios with time-invariant channel and low frequency-selectivity over the codeword length, e.g., if only a few resource blocks are scheduled. But this diversity order of 2 is only achieved with maximum likelihood (ML) decoding.

To approach ML performance efficiently, tree-search schemes known from sequential decoding have been proposed [10], e.g., sphere decoding or the M-algorithm. An important prerequisite is a smart definition of the tree which reduces the number of visited tree nodes and, thus, the complexity. It turns out that the mean square error is the more appropriate metric than the Euclidean metric with only small performance penalty, e.g. [11]. Sorting the layers based on a sorted QR-decomposition [12] or a permuted Cholesky decomposition [13] is the second key ingredient. Also the choice of the complex baseband representation or its equivalent real-valued representation as the underlying signal model makes a difference due to additional degrees of freedom for sorting in the real-valued model.

An alternative advanced MIMO receiver is serial interference cancellation (SIC), e.g., in case of a 2x2 system where two codewords are transmitted in parallel. Here, the re-encoding of the data stream detected first introduces additional latency.

In all equaliser modes, generation of LLR is necessary to provide an input to the turbo channel decoder. In particular, this is a challenge for close-to-ML MIMO equalisers and increases their complexity significantly since we do not only search for the ML solution but also for the best counter-hypothesis (assuming a max-log approximation to the problem). A simultaneous search of the tree is the current state of the art in high-throughput communication [14].

Finally, equalisation of inter-carrier interference may also become an issue for large velocities: In LTE, a reference channel model for a high-speed train scenario is defined with a Doppler of 750 Hz (5% of the carrier spacing) at 2.69 GHz carrier frequency.

D. Outer receiver

Specifically for the LTE turbo code, although its generator polynomials are the same as for the 3GPP HSPA turbo code, the turbo code internal interleaver is different. Whereas in HSPA the prunable prime interleaver (PIL) is used as the turbo internal interleaver, the so-called quadratic permutation polynomial (QPP) turbo code interleaver is standardized for the LTE [3]. With the QPP interleaver [15], the LTE turbo code has comparable or even better performances compared to the HSPA turbo code. However, the main reason for introducing a

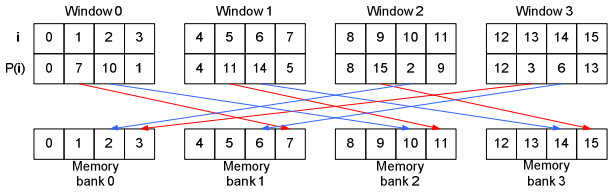

Fig. 6 Contention freeness property.

new turbo internal interleaver for LTE was to ease an implementation in hardware for achieving the high throughput (Tput) requirement.

When studying high-Tput turbo decoders that try to increase the internal parallelism used in the maximum a posteriori (MAP) constituent decoder, it turns out that the achievable Tput is limited by memory access conflicts to the 'a-priori' memory which exchanges the feedback information between the two constituent decoders. For the chosen LTE interleaver these access conflicts can be avoided and multiple parallel decoders (workers) can work on different windows of the decoding trellis at the same time. Fig. 6 illustrates the memory contention freeness property of the LTE interleaver.

As an example consider a code block of length 16 which is subdivided into 4 windows which are processed simultaneously. Whenever the i-th index (the index having fixed offset i=0,1,2,3 within each window) within two or more windows try to fetch data from the memory banks in parallel, no memory access conflicts occur, no matter whether the first constituent decoder operates on the non-interleaved data or the second decoder operates on the permuted data given by the permutation rule $P(i)$. In Fig. 6 the situation is shown in red and blue for offsets i=1 and 2, respectively. Given the nominal maximum Tput of the system (e.g. 150Mbps for a 2*2 MIMO configuration in 20 MHz bandwidth), the internal Tput requirement for the MAP constituent decoder is at least increased by the number of turbo half iterations used, i.e. 2.4 Gbps for 8 full iterations for the example configuration.

The codeblock-specific CRC which is attached in addition to the CRC over the entire payload block can serve as an early stopping criterion of the iterative turbo decoding process which helps to reduce UE power consumption.

Apart from turbo decoding and CRC checking, LTE (like HSPA) supports hybrid ARQ with incremental redundancy (IR) and soft combining at the receiver which increases robustness in addition to the link adaptation based on CQI. Compared to HSPA the rate-matching algorithm to support arbitrary code rates and IR was simplified. Fig. 7 shows the virtual buffer rate-matching used by LTE. Each bit stream (systematic, parity1 and 2) of the rate-1/3 turbo encoder output of each code block is first permuted by a subblock interleaver and organized in a virtual buffer. Equidistant entry points to this buffer mark starting positions from which data is read out from the virtual buffer for the individual redundancy versions.

On the receiver side softbits in the form of LLR are combined with those already available from previous transmissions of the same packet.

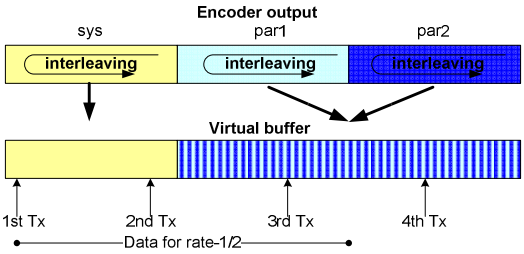

Fig. 7 Virtual buffer rate-matching.

IV. Computational Efforts and Memory Requirements

A. FFT

DFT (Discrete Fourier Transform) is the core function of OFDM demodulator which demodulates the subcarrier signal from time domain to frequency domain. The DFT can be efficiently implemented using the FFT, say, based on the well-known butterfly operations. The computational requirement of the FFT can be very high, especially for large FFT block size N which in case of the LTE can be up to 2048 complex samples. The computational complexity of the FFT with N complex samples based on a radix-2 algorithm is about $N/2 \cdot \mathrm{ld}N$ complex multiplications and $N \cdot \mathrm{ld}N$ complex additions.

B. Channel estimation

To give some insights on the complexity of the channel estimator introduced in Section II-B we focus on a 1x2 receive diversity configuration for a transmission bandwidth of 10 MHz (see also Fig. 5). Assuming a full bandwidth occupation, the number of used subcarriers is N_{data} = 600 and the number of pilots (reference symbols only) N_{pilot} = 100. As mentioned in Section III.B, in a robust implementation of the channel estimator, the interpolation coefficients are real and can be computed offline. Specifically for an example analysis, the length of the frequency and time interpolation filter was fixed to N_f = 12 and N_t = 4, respectively. The overall number of complex additions and multiplications required per subframe (14 OFDM symbols) and per transmit-receive pair is then given by (including also the initial demodulation of the pilots):

$$N_{mlk} = N_{add} = 4\left(N_{pilot} + (N_{data} - N_{pilot})N_f\right) + 10N_t N_{data} = 48400.$$

We note that $N_t = 4$ implies an initial buffering (and delay) of at least 4 OFDM symbols. In other terms, at each reference symbol, we can first perform frequency interpolation. Then, using the 4 most recent frequency estimates, we can interpolate the previous 2 or 3 OFDM symbols, depending on whether we are in the first or second reference symbol of a slot.

Alternative choices are possible for the positioning and length of the Wiener filters. For instance, the time interpolation window could be symmetrically placed around the OFDM symbol to be interpolated so as to leave 2 reference symbols to the right and 2 reference symbols to the left. Such a solution allows to more judiciously exploit the channel correlation properties. However, the buffering requirements would be higher. Similarly, longer filters can be designed for improved

noise averaging at the expenses of complexity.

C. Equalisation

Computation of the linear MMSE coefficients requires solution of one linear system of equations per subcarrier. In the 2x2 case, this is a simple task and direct matrix inversion turns out to have the smallest complexity with sufficient numerical stability [16]. In the worst case, this can be performed on 600 subcarriers for 10 MHz bandwidth, possibly in parallel, resulting in 1500 real MIPS.

For advanced MIMO equalisation, it is important to distinguish between the average and worst-case complexity. Choosing an algorithm with deterministic complexity the algorithmic effort increases approximately by a factor of 4. Efficient LLR generation with the max-log approximation for 64 QAM and linear MIMO detection requires about 500 real MIPS.

Although these tasks are highly parallelizable they constitute a challenge for a power-efficient and area optimized implementation to meet timing requirements.

D. Outer receiver

The memory requirement of the outer receiver is dominated by the HARQ buffer size which is given by the system and the number of bits used to represent a softbit (i.e. LLR). For a Cat-4 terminal, the HARQ buffer size is approximately 1.8M softbits which is used by up to 8 HARQ processes being active in parallel. The minimal buffer requirement for a high-Tput MAP decoder with parallel processors working on the decoding trellis requires storage for 3*6144 soft input LLRs and 6144 extrinsic LLRs used for information exchange during the iterative decoding process. Typically, 4 to 8 bits are enough to represent an input or an extrinsic LLR. The number 6144 is given by the maximum code block size used for LTE.

Neglecting the computational effort for the address generation for the subblock deinterleaving required for HARQ processing, the soft combining amounts to N_{data} additions for a retransmission step. In case of a newly received packet, N_{data} softbits are copied to the HARQ buffer and additional $N_{ir} - N_{data}$ softbits are 'zero-flushed', where N_{data} denotes the number of bits transmitted in a particular subframe and N_{ir} is the number of softbits reserved for the current HARQ process. The computational effort for turbo decoding is roughly given by 100 operations per decoded bit and per MAP decoder run (half iteration). The operations include additions (subtractions) and comparisons (maximum operations) of real numbers. Note that we assume here a max-log MAP decoder operating in the log-domain and dispensing with the table lookup for the correction function. Due to the high computational complexity given in the outer receiver, a software based solution is usually ruled out – at least if a standard DSP is used without special support of the operations required by trellis decoders.

V. Conclusions

In this paper, we briefly overviewed the current 3GPP LTE standard (Rel-8) and highlighted first implementation details in an LTE terminal. The sample core functional algorithms of the baseband signal processing, especially the inner receiver and the outer turbo channel decoder, were analysed. The computational efforts, memory requirements, and relevant implementation challenges were discussed. As a result, LTE terminals can be implemented with currently available semiconductor technologies. However, flexible architecture and low-complexity but high-performance algorithms are required to deal with different MIMO modes, and to ensure low power consumption and small silicon area.

Acknowledgment

The authors wish to gratefully acknowledge the support of their colleagues at Infineon Technologies. Parts of this work are carried out within the scope of the EUREKA MEDEA+ project MIMOWA, which is partly funded by the German Federal Ministry of Education and Research.

References

[1] 3GPP TR 25.913 V7.3.0 (2006-03), *Requirements for EUTRA and EUTRAN*.

[2] 3GPP TS 36.211 V8.2.0 (2008-03), *Physical Channels and Modulation*.

[3] 3GPP TS 36.212 V8.2.0 (2008-03), *Multiplexing and Channel Coding*.

[4] 3GPP TS 36.300 V8.4.0 (2008-03), *Overall Description; Stage 2*.

[5] S.M. Alamouti, "A simple transmit diversity technique for wireless communications," *IEEE JSAC*, vol. 16, no. 8, pp. 1451-1458, Oct. 1998.

[6] A. Dammann, S. Kaiser, "Standard conformable antenna diversity techniques for OFDM and its application to the DVB-T system," *Proc. IEEE GLOBECOM'01*, pp. 3100-3105, San Antonio, Nov. 2001.

[7] M. Speth, S.A. Fechtel, G. Fock, H. Meyr, "Optimum receiver design for wireless broadband systems using OFDM – part I," *IEEE Trans. Commun*., vol. 47, no. 11, pp. 1668 – 1677, Nov. 1999.

[8] M. Speth, S.A. Fechtel, G. Fock, H. Meyr, "Optimum receiver design for OFDM-based broadband transmission – part II: a case study," *IEEE Trans. Commun.*, vol. 49, no. 4, pp. 571-578, Apr. 1001.

[9] P. Hoeher, S. Kaiser, P. Robertson, "Pilot-symbol-aided channel estimation in time and frequency," *Proc. ICASSP'97*, Vol. 3, pp. 1845-848, Munich, Apr. 1997.

[10] A. Murugan, H. El Gamal, M. O. Damen, G. Caire, "A unified framework for tree search decoding: Rediscovering the sequential decoder," *IEEE Trans. Inform. Theory*, vol. 52, no. 3, pp. 933-953, March 2006.

[11] M. Joham, L. G. Barbero, T. Lang, W. Utschick, J. Thompson, T. Ratnarajah, "FPGA Implementation of MMSE metric based efficient near-ML detection," *Int. ITG Workshop on Smart Antennas*, pp. 139-146, Darmstadt, Germany, Feb. 2008

[12] D. Wübben, R. Böhnke, V. Kühn, K. D. Kammeyer, "MMSE extension of V-BLAST based on sorted QR-decomposition," *Proc. IEEE VTC 2003 Fall*, pp. 508-512, Orlando, USA, Oct. 2003

[13] K. Kusume, M. Joham, W. Utschick, G. Bauch, "Cholesky facotrization with symmetric permutation applied to detecting and precoding spatially multiplexed data streams," *IEEE Trans. Signal Proc.*, vol. 55, no. 6, pp. 3089-3103, June 2007.

[14] E. Zimmermann, G. Fettweis, D. L. Milliner, J. R. Barry, "A parallel smart candidate adding algorithm for soft-output MIMO detection," *Proc. Int. Conf. on Source and Channel Coding*, Ulm, Germany, Jan. 2008

[15] O.Y. Takeshita, "On maximum contention-free interleavers and permutation polynomials over integer rings," *IEEE Trans. Inform. Theory*, vol. 52, no. 3, pp. 1249-1253, March 2006.

[16] J. Eilert, D. Wu, D. Liu, "Efficient complex matrix inversion for MIMO software defined radio," *Proc. ISCAS'07*, pp. 2610-2613, New Orleans, May 2007.

Note:

3GPP documents are available at http://www.3gpp.org/ftp/Specs/archive